

# Chemical Science



**Accepted Manuscript** 

This article can be cited before page numbers have been issued, to do this please use: K. Kar, G. Joshi, E. D. Jemmis and S. Ghosh, *Chem. Sci.*, 2025, DOI: 10.1039/D5SC06992K.



This is an Accepted Manuscript, which has been through the Royal Society of Chemistry peer review process and has been accepted for publication.

Accepted Manuscripts are published online shortly after acceptance, before technical editing, formatting and proof reading. Using this free service, authors can make their results available to the community, in citable form, before we publish the edited article. We will replace this Accepted Manuscript with the edited and formatted Advance Article as soon as it is available.

You can find more information about Accepted Manuscripts in the <u>Information for Authors</u>.

Please note that technical editing may introduce minor changes to the text and/or graphics, which may alter content. The journal's standard <u>Terms & Conditions</u> and the <u>Ethical guidelines</u> still apply. In no event shall the Royal Society of Chemistry be held responsible for any errors or omissions in this Accepted Manuscript or any consequences arising from the use of any information it contains.



View Article Online DOI: 10.1039/D5SC06992K

emical Science Accepted

# **ARTICLE**

# All-Boron Analogue of Planar Benzene on an Osmium Template

Ketaki Kar, a Gaurav Joshi, b Eluvathingal D. Jemmis, \*b and Sundargopal Ghosh\*a

Received 00th January 20xx, Accepted 00th January 20xx

DOI: 10.1039/x0xx000000x

The synthesis of planar hexaborane  $B_6$  ring remains a long-standing and elusive ambition in boron chemistry, defying boron's intrinsic electron deficiency that drives it to favour polyhedral three-dimensional geometries rather than chains and rings. Owing to this domination, earlier attempts to stabilize the planar  $B_6$  ring in a monometallic template encountered no success. Herein, we report the synthesis and structure of bis-nido- $[Cp^*Os(\eta^6-B_6H_{11})]$  ( $Cp^* = \eta^5-C_5Me_5$ ) (1), the first planar  $[B_6H_{11}]$  ring stabilized by monometallic late transition metal (TM) fragment,  $[Cp^*Os]$ . The fluxionality due to rapid exchange between the bridging hydrogens in 1 led to considerable structural intrigue, resembling the dynamic behaviour seen in nido- $[B_6H_{10}]$ . Furthermore, we have successfully isolated the intermediate boron chains, nido-arachno- $[Cp^*Os(\eta^6-B_5H_{12})]$  (2) and nido-arachno- $[Cp^*Os(\eta^4-B_4H_9)]$  (3). The  $B_5$  chain in 2 and the  $B_4$  chain in 3 are isoelectronic with the pentadienyl radical ( $C_5H_7$ ) and the 1,3-butadiene radical cation ( $C_4H_6$ )\*, respectively. Extensive multicenter bonding interactions are demonstrated to stabilize the unique flat ring as well as boron chains within monocapped scaffolds.

#### Introduction

The influence of planar organic aromatic molecules in chemistry is overwhelming; in contrast, the chemistry of aromatic molecules from neighbouring main group elements is only beginning. Interest in the chemistry of the  $cyclo-P_n$  ring, isoelectronic to cyclo-(CH)<sub>n</sub>, is coming of age.<sup>1-5</sup> There are now several examples of aromatic systems among heavier elements in the nitrogen group. 6-11 The boron group presents a different scenario due to electron deficiency. 12-18 The classical closopolyhedral boranes  $(B_nH_n)^{2-}$  follow Wade's Rule and the Rudolph diagram exemplify the nido- or arachno-structures with an increasing number of electrons. 12 Planar rings are rarely in the reckoning. Interestingly, the early synthesis and structural assignment of a dication of hexamethylbenzene, (C<sub>6</sub>(CH<sub>3</sub>)<sub>6</sub>)<sup>2+</sup> (I), which is isoelectronic to nido-[B<sub>6</sub>H<sub>10</sub>] (II), have been a reminder of the lineage to planar rings (Chart 1).19-22 Over the past few decades, there have been several reports on planar  $B_n$  rings (n = 3-5) stabilized either by main group or transition metal (TM) fragments. For example,  $B_3$  rings in  $Na_4[B_3(NCy_2)_3]_2 \cdot 2DME$  (III) (Chart 1),  $B_4$  ring in [(CO)<sub>3</sub>Fe( $B_4H_8$ )],  $B_5$  ring in [CpFe( $B_5H_{10}$ )] and others.<sup>24-30</sup> Although numerous theoretical studies have shown the stabilization of the planar B<sub>6</sub> ring isoelectronic with benzene,31-35 only a very few experimental reports have demonstrated its stabilization within a triple-decker sandwichtype scaffold using early transition metals. 36-39 Recently, we

Although some reports on planar  $B_n$  (n=4 and 5) rings stabilized in monometallic templates are available, all attempts to isolate a hexagonal planar  $B_6$  ring in a monometallic template have not met with success. In this article, we report the first planar  $B_6$  ring stabilized by a monometallic {Cp\*Os} in bis-nido-arrangement, [Cp\*Os-( $\eta^6$ -B<sub>6</sub>H<sub>11</sub>)] (1), utilizing an optimized new synthetic strategy involving controlled pyrolysis (Scheme 1). The [B<sub>6</sub>H<sub>11</sub>] ring with five B-H-B-bridging hydrogens is isoelectronic to benzenyl cation radical [C<sub>6</sub>H<sub>6</sub>]\*. In pursuit of elucidating the intermediates from monoborane precursor to complex 1

**Chart 1.** The occurrence of pyramidal geometry in  $(C_6(CH_3)_6)^{2+}$  (I), isoelectronic to *nido*- $B_6H_{10}$  (II), planar  $B_3$  rings in  $Na_4[B_3(NCy_2)_3]_2 \cdot 2DME(III)$ .

have compiled these significant experimental and theoretical advances and proposed a modified Rudolph diagram with emphasis on planar boron rings.  $^{30}$  Despite several significant efforts and occasional breakthroughs in the chemistry of hexagonal planar boron rings, the isolation of the flat parent  $B_6$  ring, isoelectronic to benzene, in a monometallic template remains enigmatic.

<sup>&</sup>lt;sup>a.</sup> Department of Chemistry, Indian Institute of Technology Madras Chennai 600036, India E-mail: sghosh@iitm.ac.in.

b. Inorganic and Physical Chemistry Department, Indian Institute of ScienceBangalore 560012, IndiaE-mail: jemmis@iisc.ac.in.

<sup>†</sup> Footnotes relating to the title and/or authors should appear here.

Supplementary Information available: CCDC 2438685 (for 1), 2438887 (for 2), 2438789 (for 3).

For ESI and crystallographic data in CIF or other electronic format see DOI See DOI: 10.1039/x0xx00000x

ARTICLE Journal Name

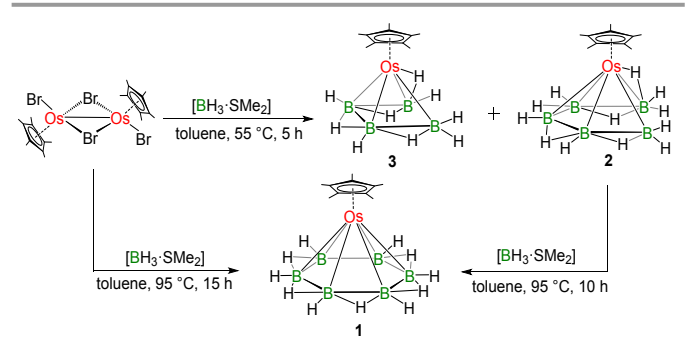
featuring a flat  $B_6$  ring, we have also isolated key intermediates nido-arachno- $[Cp^*Os(\eta^5-B_5H_{12})]$  (2) and nido-arachno- $[(Cp^*Os)(\eta^4-B_4H_9)]$  (3). The  $[B_5H_{12}]$  in 2 and  $[B_4H_9]$  in 3 are isoelectronic to pentadienyl radical  $[C_5H_7]$ , and 1,3-butadiene radical cation  $[C_4H_6]^{+}$ , respectively, using less obvious analogies ( $vide\ infra$ ). Although attempts to isolate the  $B_2$  and  $B_3$  intermediates have not been successful, this is the first synthetic attempt to follow reactions starting from  $B_1$  species to the planar  $B_6$  ring, isolating and characterizing the intermediate  $B_4$  and  $B_5$  chains along the way. Complexes 1, 2, and 3 have been well-characterized through various spectroscopic techniques and single-crystal X-ray diffraction analysis.

### Results and discussion

#### Synthesis and Characterization

The thermolysis reaction of [Cp\*OsBr<sub>2</sub>]<sub>2</sub> with an excess of [BH<sub>3</sub>·SMe<sub>2</sub>] at 95 °C resulted in the formation of [Cp\*Os( $\eta^6$ -B<sub>6</sub>H<sub>11</sub>)] (1) as a colourless solid along with some unidentified air and moisture-sensitive products. The <sup>1</sup>H NMR spectrum of 1 shows a peak at  $\delta$  = 1.58 ppm for Cp\* that was confirmed by <sup>13</sup>C{<sup>1</sup>H} NMR. The <sup>1</sup>H chemical shift at  $\delta$  = -3.56 ppm indicates B-H-B protons. The room-temperature <sup>11</sup>B{<sup>1</sup>H} NMR spectrum of 1 exhibits a single peak at  $\delta$  = 8.6 ppm. The <sup>1</sup>H{<sup>11</sup>B} chemical shift at  $\delta$  = 3.56 ppm can be assigned to six terminal B–H<sub>t</sub> protons. The mass spectrum of 1 shows isotopic distribution patterns at m/z 402.2301, corresponding to the molecular formula [C<sub>10</sub>H<sub>27</sub>B<sub>6</sub>Os].

To corroborate the spectroscopic data, a single-crystal X-ray diffraction analysis was carried out on a suitable crystal of 1. The molecular structure of 1, shown in Figure 1, shows a planar sixmembered  $B_6$  ring stabilized by a monometallic {Cp\*Os} unit. There are six terminal B-H bonds and an additional six hydrogens are positioned to bridge the six B-B bonds forming a [B<sub>6</sub>H<sub>12</sub>] motif with a symmetrical environment. The average Os-B bond distance (2.187 Å) is comparable with the previously reported osmaboranes.40 The average B-B bond distance of 1.753 Å in **1** is comparable with reported triple-decker sandwich nido-closo-nido- $[(Cp*Re)(\mu-\eta^6:\eta^6-1,2-B_6H_4Cl_2)(Cp*$ Re)]<sup>36</sup> (1.726 Å) but slightly shorter than *nido-closo-nido-* $[(Cp*Ti)(\mu-\eta^6:\eta^6-B_6H_6)(\mu-H)_6(Cp*Ti)]^{37}$  (1.80 Å). The average ∠B-B-B angle in the six-membered ring is 119.98°, similar to that of a planar hexagon (120°). The molecular formula deduced from the crystal structure, i.e.,  $[Cp*Os(\eta^6-B_6H_{12})]$  leads to an electron count around the metal of 19 (1×{Cp\*Os} = 13, {B<sub>6</sub>H<sub>12</sub>}



**Scheme 1.** Synthesis of **1** [Cp\*Os( $\eta^6$ -B<sub>6</sub>H<sub>11</sub>)], **2** [Cp\*Os( $\eta^5$ -B<sub>5</sub>H<sub>12</sub>)], and **3** [Cp\*Os( $\eta^4$ -B<sub>4</sub>H<sub>9</sub>)].

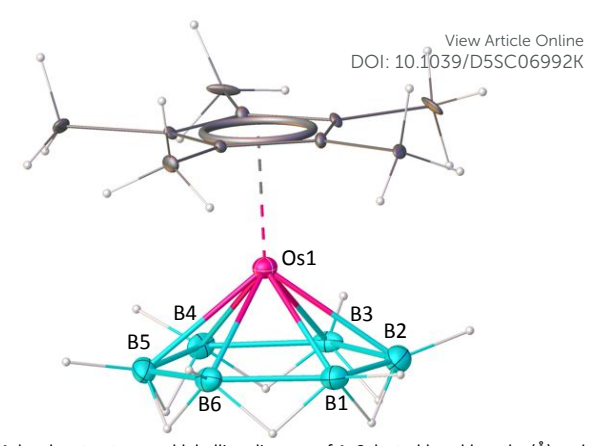


**Figure 1.** Molecular structure and labelling diagram of **1.** Selected bond lengths (Å) and angles (deg): B1-B2 1.754(17), B2-B3 1.74(3), B3-B4 1.75(2), B4-B5 1.762(14), B5-B6 1.74(2), Os1-B1 2.26(3), Os1-B3 2.20(2), Os1-B5 2.16(3); B4-B5-B6 117(2), B3-B4-B5 123(2). The standard refinement of the X-ray diffraction data for this 18-electron complex **1** indicates the presence of six bridging hydrogens (B-H-B). However, for a neutral 18-electron complex, only 5 bridging hydrogens are expected. Closer analysis of the X-ray diffraction data, supported by theoretical calculations, confirms a structure featuring five bridging hydrogens, as discussed in the text.

= 6), suggesting the presence of an odd electron. However, no paramagnetic behaviour was observed in the EPR spectrum of **1**. Also, computational studies of the structure [Cp\*Os( $\eta^{6}$ -B<sub>6</sub>H<sub>12</sub>)], at the B3LYP-D3/Def2-SVP level of theory, with the odd electron, led to a non-planar B<sub>6</sub> ring (Figure S29). Further, there is no evidence of the presence of an anion in the unit cell of 1. We examined the X-ray diffraction data further. The terminal B-H and bridging B-H-B protons were identified from difference electron density maps, and their positions were refined using single-crystal X-ray analysis. It was found that all the bridging hydrogen sites are partially occupied with equal occupancy. This partial occupancy indirectly suggests the presence of five bridging hydrogen atoms in 1. Therefore, it is reasonable to assume that the correct formula for **1** is  $[Cp*Os(\eta^6-B_6H_{11})]$ , which results in an 18-electron count around the osmium center (13 electrons from  $\{Cp*Os\}$  and 5 from the  $\{B_6H_{11}\}$ ).  $[B_6H_{11}]$  is isoelectronic to benzenyl cation radical  $[C_6H_6]^+$ , a  $5\pi$  ligand. The five additional hydrogens bridge the five out of six B-B bonds and contribute the necessary five electrons. As expected, the non-bridged 2center-2electron (2c-2e) B-B bond is computed to be shorter (1.635 Å at B3LYP-D3/Def2-SVP level) than the bridged 3c-2e B-H-B bond (1.761-1.808 Å, Figure S30a, Table S1). The distribution of molecules in the crystal structure is such that the position of the B-B bond without bridging hydrogen in the crystal structure, is random, resulting in diffraction data supporting nearly equal B-B bond distances. The sixth 2c-2e B-B bond is also capable of forming a similar bridged B-H-B 3c-2e bond. Therefore, to check the fluxionality of complex 1, variable temperature <sup>1</sup>H and <sup>11</sup>B{<sup>1</sup>H} NMR experiments were performed (Figures 2a and 2b), enabling the possibility of slowing down the exchange of five bridged hydrogen atoms. But this experiment revealed no splitting of the single 11B peak except broadening at lower temperatures This broadening may be due to the lessening of spin-lattice relaxation time, a common phenomenon for boron-containing complexes. Probably, a rapid hydrogen exchange among the bridging hydrogens in

emical Science Accepted Manuscrip

View Article Online DOI: 10.1039/D5SC06992K

# **ARTICLE**

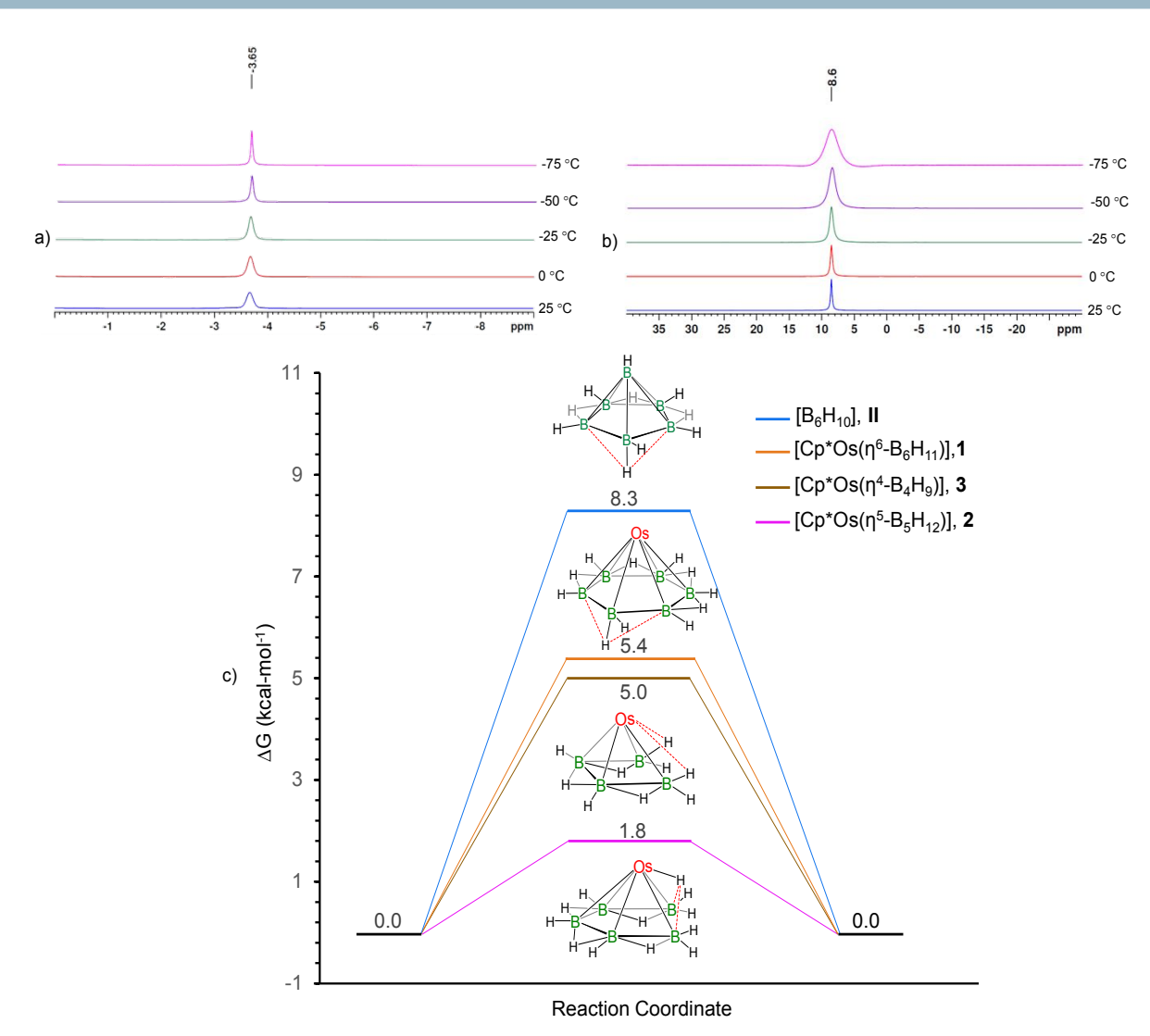


Figure 2. a) Variable-temperature  ${}^{11}H^{11}B$ } NMR spectrum of 1 in the hydride region showing no splitting; b) Variable-temperature  ${}^{11}B^{1}H$ } NMR spectra of 1 showing no splitting except broadening at lower temperatures. c) Free energy surface for the terminal and bridging hydrogen exchange in  $[B_6H_{10}]$  (II) and  $[Cp^*Os(\eta^6-B_6H_{11})]$  (1), the switching of B-H-Os bridge from one boron to another in  $[Cp^*Os(\eta^6-B_6H_{12})]$  (2), and the switching of agostic interaction in  $[Cp^*Os(\eta^6-B_6H_{12})]$  (3) at the B3LYP-D3/Def2-SVP level of theory with implicit solvation at 298K. For easy comparison of the variation in the barrier for hydrogen shift, the relative energies of the ground states of all compounds are brought to zero in the Figure.

solution led to the equivalence of five bridging hydrogens. Such a type of rapid exchange of bridging hydrogens has been reported in [nido-B<sub>6</sub>H<sub>10</sub>] (II), producing similar ambiguities.<sup>21</sup> The barrier for exchange of bridging hydrogens in **1** is calculated to be 5.4 kcal/mol, much lower than the corresponding barrier for II [nido-B<sub>6</sub>H<sub>10</sub>] (8.3 kcal/mol) at the same level of theory (Figure 2c). Therefore, due to the very high fluxionality of the bridging hydrogen atoms, the expected splitting in the variable-temperature <sup>11</sup>B and <sup>1</sup>H NMR experiments was not observed, even at very low temperatures. It is due to the difficulty in locating the light H atom among a cluster of heavier atoms,

together with the possibility of random positioning of the five bridging H-atoms in the  $B_6$  ring in the crystal structure, leading to the diffraction data that gave six bridging hydrogens instead of five.

#### **Intermediates**

To gain insights into the formation of  $\mathbf{1}$ , the reaction of  $[Cp^*OsBr_2]_2$  with  $[BH_3 \cdot SMe_2]$  was monitored under various reaction conditions. We observed that at milder reaction conditions, we could isolate the lower boron congeners  $[Cp^*Os(\eta^5-B_5H_{12})]$  (2) and  $[(Cp^*Os)(\eta^4-B_4H_9)]$  (3). Further thermolysis of the mixture of  $\mathbf{2}$  and  $\mathbf{3}$  in the presence of

Science Accepted Manuscr

[BH<sub>3</sub>·SMe<sub>2</sub>] at 95 °C for 10 h resulted in the formation of **1**. The  $^1$ H NMR spectrum showed peaks at  $\delta=1.48$  ppm (**2**) and 1.56 ppm (**3**) for Cp\* protons. Peaks in  $^1$ H{ $^{11}$ B} NMR at  $\delta=-3.36$  and -3.89 ppm in 2:2 ratio (for **2**) and  $\delta=-3.79$  and -4.16 ppm in 1:2 ratio (for **3**) correspond to different B-*H*-B protons. The upfield  $^1$ H chemical shifts at  $\delta=-12.55$  and -15.60 ppm may correspond to terminal Os-*H* or Os-*H*-B protons, which were further confirmed by  $^1$ H- $^{11}$ B HSQC as Os-*H*-B protons (Figures S14 and S24). The room-temperature  $^{11}$ B{ $^1$ H} NMR spectrum of **2** exhibited peaks at  $\delta=2.9$ , 0.8 and -6.5 ppm in 2:1:2 ratio, while **3** exhibited peaks at  $\delta=-2.5$  and -12.1 ppm in 2:2 ratio. The mass spectra of **2** and **3** demonstrated isotopic distribution patterns at m/z 390.2105 and 419.2204, respectively.

The solid-state X-ray structure of 2 confirmed that a B<sub>5</sub> chain is stabilized in the coordination sphere of {Cp\*Os} unit and this is best described as nido-arachno arrangement (Figure 3). The average B-B bond distance of 1.822 Å is considerably longer than the average B-B bond distance of 1.713 Å in the tripledecker sandwich complex [(Cp\*W)<sub>2</sub>B<sub>5</sub>H<sub>9</sub>].<sup>41</sup> Unfortunately, due to the presence of two-fold disorder, it was not possible to locate or freely refine any of the 12 hydrogens associated with Os-H-B, B-H-B and B-H<sub>t</sub>. Thus, the hydrogen positions were inferred based on various NMR experiments (Figures S10, S13 and S14) and computational studies (Figure S30b). Interestingly, the [B<sub>5</sub>H<sub>12</sub>] chain in 2 is isoelectronic to pentadienyl radical,  $[C_5H_7]$ , a  $5\pi$  ligand. This isoelectronic equivalence is most easily demonstrated by assuming [C5H7] as an anion [C5H7] with  $6\pi$ electrons as in [Cp]<sup>-</sup>. Replacement of five carbon atoms in [C₅H<sub>7</sub>]<sup>-</sup> by five isoelectronic  $[B]^-$  units results in the formula  $[B_5H_7]^{6-}$ . The four B-B sigma bonds can be protonated so that the charge is reduced to -2 in [B<sub>5</sub>H<sub>11</sub>]<sup>2-</sup>. If one of the end [BH<sub>2</sub>] groups (say B1) is also protonated, the resulting [B<sub>5</sub>H<sub>12</sub>] will have the end boron as an equivalent of  $[BH_4]^-$ . Thus, there are four  $\pi$  electrons from B2 to B5 and two electrons from one of the B-H bond pairs of B1 to constitute the 6 electrons equivalent of [Cp]-. The computed structure clearly indicates a stretched B1-H-Os1 interaction, where the B1-H bond is long (1.482 Å at B3LYP-

D3/Def2-SVP) and the Os1-H distance of 1.657 Å is comparable to the metal-hydride bond distance of 104.9666 $[Os(PPh_3)_2H_2(\eta^4-B_4H_8)].^{29}$  The distance between the hydrogen of the B5-H-Os1 3c-2e bond and the terminal B5 atom, i.e., B5-H, is 1.966 Å. If the protonation is assumed to take place at that end (B5), there will be an equivalent structure with B5-H-Os1 3c-2e bond. The barrier for the interconversion between these two equivalent structures is calculated to be only 1.8 kcal/mol (Figure 2c). A similar phenomenon was observed with arachno-[B<sub>5</sub>H<sub>11</sub>].<sup>22</sup> Due to this very fast exchange, the expected change in the variable-temperature <sup>11</sup>B and <sup>1</sup>H NMR experiments was not observed, even at very low temperatures (Figures S16 and S17). The crystal structure presents a more complex picture. The structure has a two-fold disorder in the ratio 38:62. With the disorder and a very heavy osmium atom present, it is impossible to locate the hydrogen atoms belonging to borons from the difference Fourier map and these hydrogens cannot be fixed geometrically. This explains the unusual differences in B-B bond lengths from the X-ray and computational data (Table S1). Although an analogous C<sub>5</sub> chain was observed in [Cp\*Ru( $\eta^5$ - $C_5H_7(CH_3))]^{+,42}$  **2** is the first example of boron catenation resulting in the formation of a B<sub>5</sub> chain in the coordination sphere of a monometallic {Cp\*Os} unit.

The solid-state X-ray structure of **3** showed a B<sub>4</sub> chain stabilized in the coordination sphere of a monometallic {Cp\*Os} unit and can be described as *nido-arachno* arrangement (Figure 3). The average B-B bond distance is 1.841 Å is comparable to the average B-B bond distance in [W(IMes)( $\eta^4$ -BH<sub>2</sub>Mes-BMes-BMes-BMes-BH<sub>2</sub>Mes)] (1.82 Å)<sup>43</sup>. This molecule contains nine hydrogens which are linked as Os-*H*-B, B-*H*-B, and terminal B-H bonds. Among these, five are terminal, three bridge the B1-B2, B2-B3, and B3-B4 bonds and one bridges the Os1-B1 bond (Figure 3). Though Fehlner and co-workers previously characterized a iridium-stabilized B<sub>4</sub> chain [(Cp\*Ir)B<sub>4</sub>H<sub>10</sub>], only by NMR experiments,<sup>44</sup> **3** is the first example of a structurally characterized osmium-stabilized B<sub>4</sub> chain. The coordinated [B<sub>4</sub>H<sub>9</sub>] chain in **3** is isoelectronic to 1,3-butadiene radical cation

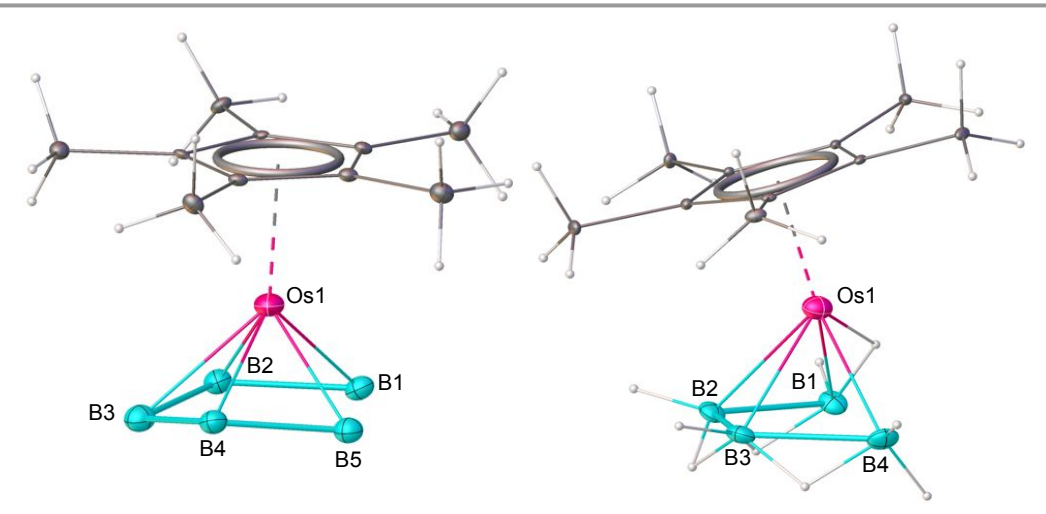


Figure 3. Molecular structures of (2)  $Cp^*Os(\eta^5-B_5H_{12})$  (left) and (3)  $(Cp^*Os)(\eta^4-B_4H_9)$  (right). Hydrogen positions in 2 could not be located crystallographically due to disorder. They were confirmed by different NMR experiments and computational analysis. Selected bond lengths [Å] and angles (deg) (2): Os1-B2 2.02(3), Os1-B3 2.15(3), Os1-B5 2.16(3), Os1-B4 2.23(3), Os1-B1 2.24(3), B1 B2 1.77(4), B3 B4 1.77(4); B2 Os1 B3 57.0(12), B3 Os1 B5 81.9(17), B1 B2 B3 118(3), B4 B3 B2 118(3), B5 B4 B3 107(3). (3): B1-B2 1.846(11), B2-B3 1.826(12), B3-B4 1.851(13), Os1-B1 2.305(7), Os1-B2 2.146(7), Os1-B3 2.150(7), Os1-B4 2.300(7); B3 B2 B1 111.7(6), B2 B3 B4 112.4(5).

View Article Online DOI: 10.1039/D5SC06992K

# **ARTICLE**

 $[C_4H_6]^+$ , a  $3\pi$  ligand which, in addition, may donate two electrons through an agostic B-H-Os bond. Replacement of four carbon atoms by four isoelectronic [B]- units results in the formula [B<sub>4</sub>H<sub>6</sub>]<sup>3-</sup>. Protonation of the three B-B sigma bonds results in the neutral [B<sub>4</sub>H<sub>9</sub>]. The three bridging hydrogens provide three electrons. A terminal B-H bond from one of the two end [BH<sub>2</sub>] groups (say B1) of the B<sub>4</sub>-chain provides an additional two electrons through the agostic B1-H-Os1 interaction (B1-H = 1.338 Å, Os1-H = 1.797 Å, Os1-B1 = 2.015 Å, Figure S33). The other [BH<sub>2</sub>] group (say B4) is similarly capable of this interaction, resulting in a degenerate exchange between the terminal boron atoms with an energy barrier of 5.0 kcal/mol (Figure 2c). Due to this rapid exchange of Os-H-B bridging hydrogen, no change was observed in the variable-temperature <sup>11</sup>B and <sup>1</sup>H NMR (Figures S26 and S27), similar to that of complexes 1 and 2. While catenation and chain structures serve as the foundation of organic chemistry, homonuclear chains in the chemistry of boron are very limited.<sup>43</sup> Instead, the formation of hypervalent clusters and cages is the norm. Thus,

the  $\pi\text{-type}$  complexes featuring  $B_5$  and  $B_4$  chain units are very novel.

Our attempts to isolate intermediates with two and three boron atoms ( $B_2$  and  $B_3$ ) were not successful in this reaction pathway. Generally, in most of the metathesis reactions between pentamethylcyclopentadienyl metal polychlorides and borane/borate reagents, such as [BH3·THF], [BH3·SMe2], [LiBH4], Li[BH<sub>3</sub>(EPh)], (E = S, Se or Te) etc., the typical by-products are [BH<sub>3</sub>], [BHCl<sub>2</sub>], [BH<sub>2</sub>Cl] etc. All these reagents underwent saltelimination reactions leading to the formation of metal polyborohydride complexes that successively vielded metallaborane by hydrogen elimination.<sup>45,46</sup> So, in this case, the metathesis reactions between pentamethylcyclopentadienyl metal polybromides and [BH<sub>3</sub>·SMe<sub>2</sub>] may have primarily yielded [BH<sub>3</sub>], [BHBr<sub>2</sub>], [BH<sub>2</sub>Br] etc., along with osmium polyborohydride complexes, which may have undergone hydrogen elimination to form these complexes 2, 3, and subsequently, 1. In addition,

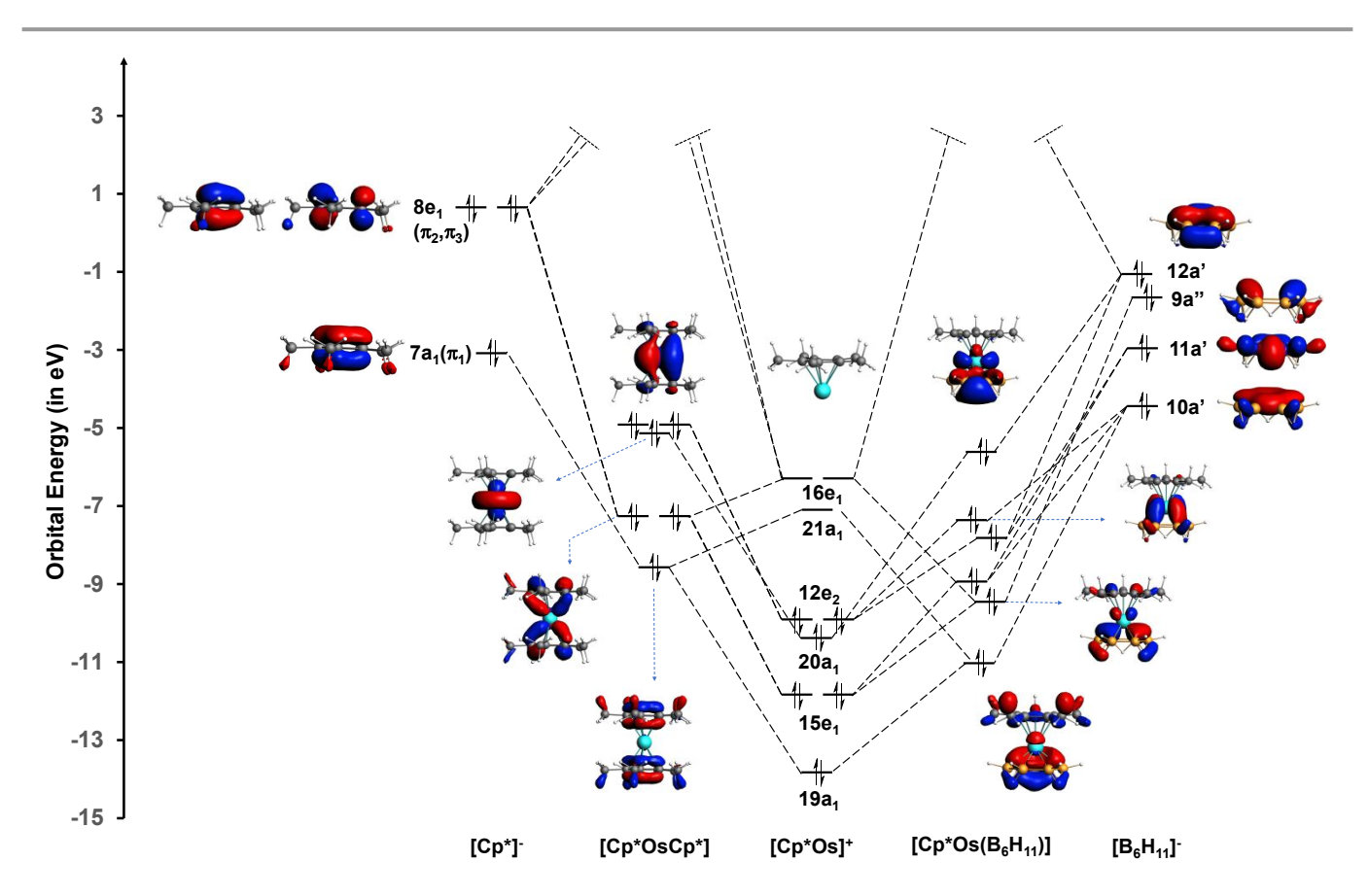


Figure 4. Orbital interaction diagram of  $\{Cp^*Os\}^+$  with  $\{C_{p^*}\}^-$  and  $\{B_6H_{11}\}^-$  ligands in complex  $[Cp^*OsCp^*]$  and 1,  $[Cp^*OsB_6H_{11}]$  in  $C_{5v}$  and  $C_5$  symmetry respectively computed at B3LYP-D3/TZP level of theory using ADF software.  $^{49,50}$  The well-known frontier orbitals of the fragment  $[Cp^*Os]$  are given in the middle of the diagram. Only the occupied  $\pi$  MOs of  $Cp^*$  are

given on the left. The top four frontier MOs are given for  $[B_6H_{11}]$  on the extreme right and there is extensive  $\sigma$ - $\pi$  mixing in  $[B_6H_{11}]$ .  $C_{5\nu}$  point group nomenclature  $[B_6H_{11}]$ .  $C_{5\nu}$  point group nomenclature  $[B_6H_{11}]$ . In 1, the  $\sigma$ - $\pi$  mixing makes the distinction between  $\sigma$  and  $\pi$  orbitals difficult, unlike  $[Cp^*OSCp^*]$ .

DOI: 10.1039/DSSC06992K

these reactions also yielded several air and moisture-sensitive by-products. Although we have tried to isolate other sensitive by-products by fractional crystallization, we were unsuccessful mainly due to their poor yields. We could isolate only those compounds that are stable during chromatography work-up. This prevents us from formulating an acceptable reaction mechanism currently.

#### **Electronic Structures and Bonding**

This article is licensed under a Creative Commons Attribution 3.0 Unported Licence.

Open Access Article. Published on 24 Oktober 2025. Downloaded on 26/10/2025 15.26.27.

While the electron requirement of  ${\bf 1}$  is understood in comparison to ferrocene, these structures, especially  ${\bf 2}$  and  ${\bf 3}$ , are better understood using the mno rule, an extension of Wade's Rule. <sup>47</sup> According to this, the electron count required for the stability of a condensed polyhedral structure is given by (m + n + o) skeletal electron pairs, where m is the number of polyhedra, n is the number of vertices, and o is the number of polyhedra connected through a single bridging atom. For *nido* and *arachno* arrangements, two additional variables, p and q,

are added, with values of 1 and 2 electron pairs, respectively. Thus, ferrocene requires 16 (m = 2, n = 11, o = 1, p = 2) skeletal electron pairs. What is available is 16 (30 electrons from ten [CH], and 2 electrons from Fe), so that ferrocene is electron sufficient. Application of the mno rule demands 17 electron pairs in 1 (m = 2, n = 12, o = 1 and p = 2). What is available is also 17 (15e from five [CH], 12e from [B<sub>6</sub>H<sub>6</sub>], 5e from five bridging H, and 2e from Os). It is instructive to relate the bonding in 1 to the known triple-decker sandwich nido-closo-nido-[(Cp\*Re)(μ- $\eta^6$ :  $\eta^6$ -1,2-B<sub>6</sub>H<sub>4</sub>Cl<sub>2</sub>)(Cp\*Re)]. While an mno electron count of 25 electron pairs (m = 3, n = 18, o = 2 and p = 2) is obtained for a compound *nido-closo-nido-*[(Cp\*Re)( $\mu$ - $\eta$ <sup>6</sup>: $\eta$ <sup>6</sup>-B<sub>6</sub>H<sub>6</sub>) (Cp\*Re)], the available electron pairs are only 22 (15 from two Cp\*, 6 from the [B<sub>6</sub>H<sub>6</sub>] ring and one from the Re atoms together assuming a pseudo octahedral complex with d<sup>6</sup> Re atoms). However, the number of electrons required for stability in triple-decker complexes depends on many factors such as the size of the middle ring, the size of the metal atom, substituents

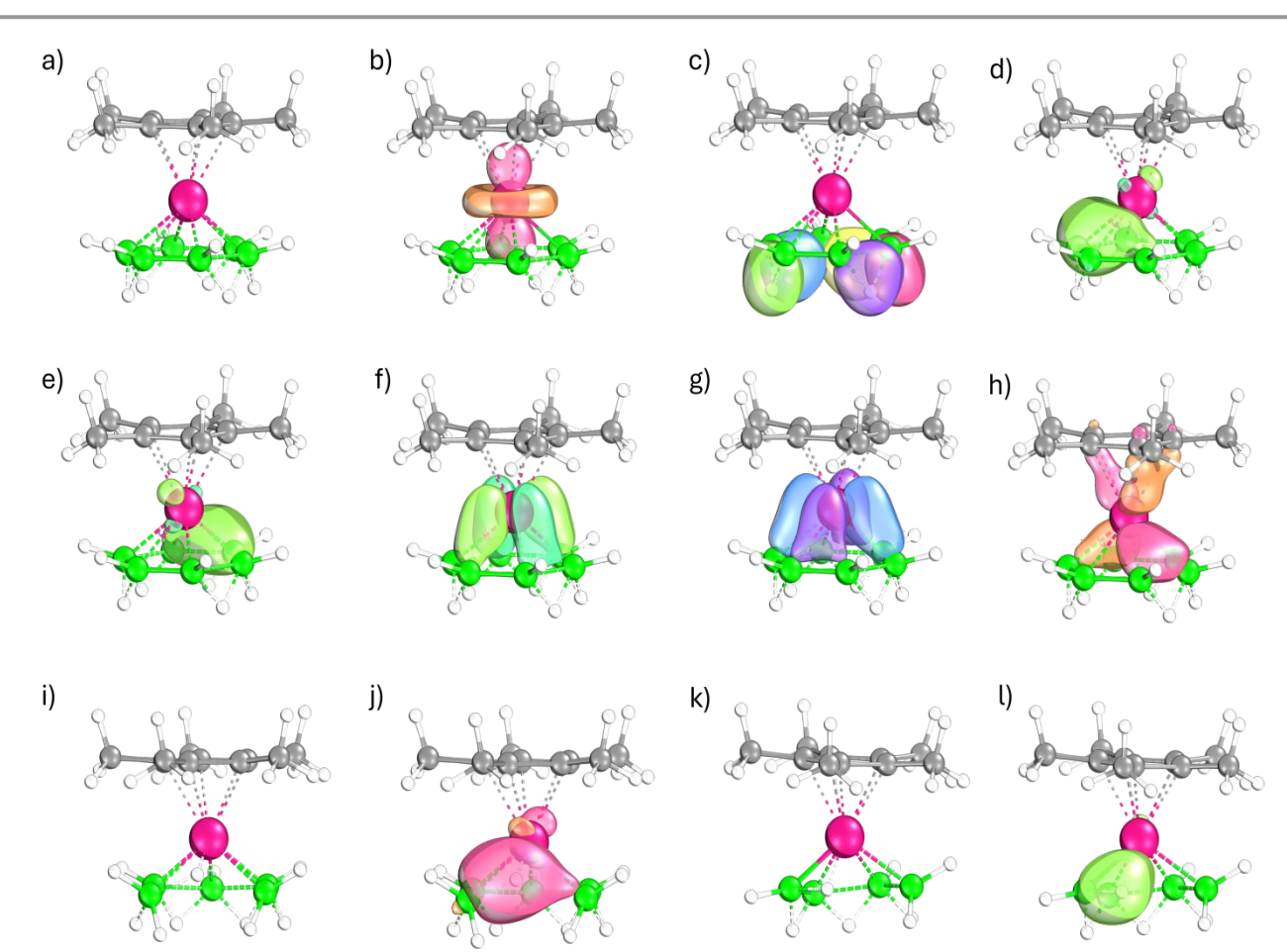


Figure 5. Selected localized orbitals of 1 (a) computed using IBOview: (b) a 1c-2e lone pair on osmium; (c) five 3c-2e bond orbitals; and (d-h) five multicenter osmium-boron bond orbitals. Complex 2 (i) and 3 (k) display similar localized orbitals, with the exception that in each case one of the five osmium-boron multicenter orbitals include contribution from a terminal hydrogen (j and I, respectively). For clarity, the 2c-2e bond orbitals, and three metal-Cp\* multicenter orbitals are omitted (see text).

on the rings, metal-metal bond, spin multiplicity of the complex etc.<sup>48</sup> These variables disappear when one of the [Cp\*Re] groups is removed, leading to the equivalent of **1**.

The osmaborane **2** has a *nido*-[Cp\*Os] and an *arachno*-[OsB<sub>5</sub>H<sub>12</sub>] condensed through Os, so that the mno rule gives 17e pairs (m = 2, n = 11, o = 1, p = 1, q = 2). The number of skeletal

Open Access Article. Published on 24 Oktober 2025. Downloaded on 26/10/2025 15.26.27.

Journal Name ARTICLE

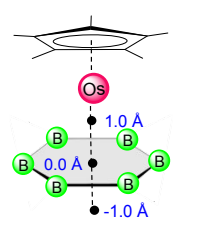
electron pairs available is also 17 (15 electrons from five [CH], 10 electrons from [B $_5$ H $_5$ ], 4 electrons from four bridging H, 2 electrons from the two additional H on the terminal B atoms, 1 electron from the additional H atom forming the Os-H-B 3c-2e bridge and 2 electrons from Os). The mno count for **3**, (Cp\*Os)( $\eta^4$ -B $_4$ H $_9$ ), is 16 skeletal pairs (m = 2, n = 10, o = 1, p = 1, and q = 2). What is available appears to be only 15 (15 electrons from five [CH], 8 electrons from [B $_4$ H $_4$ ], 3 electrons from three bridging H, 2 electrons from two additional H on the terminal B atoms and 2 electrons from Os). However, a closer look at the structure indicates that one of the terminal B-H bonds of the arachno-[OsB $_4$ H $_9$ ] unit bends towards the metal, making it an agostic-B-H-Os interaction. This completes the required electronic requirement.

While this qualitative electron counting brings equivalence between the electronic structure of permethylferrocene and that of  $[Cp^*Os(\eta^6-B_6H_{11})]$  **1,** there are many differences in detail. The high stability of the C-C  $\sigma$  bond in Cp\* and the high symmetry keep a large difference in the  $\pi$  and  $\sigma$  bond orbitals in Cp\*. In contrast, the five B-B bridging hydrogens in  $[B_6H_{11}]$  force the terminal hydrogens on the opposite side of the  $B_6$  ring. This leads to  $\sigma$ - $\pi$  mixing and the distinction between  $\pi$  and  $\sigma$  MOs vanishes. The consequences are seen in Figure 4, where fragment interaction diagrams for the formation of permethylosmocene and structure **1** are compared. While it is still possible to trace the MOs with dominant contribution of  $\pi$  MOs of Cp\* in permethylosmocene, it is not easily possible to make the distinction between orbitals with predominant  $\sigma$  or  $\pi$  interaction in structure **1**,  $[Cp^*Os(\eta^6-B_6H_{11})]$ .

The bonding of **1**, **2**, and **3** is further examined using Intrinsic Bond Orbitals (IBOs).<sup>51,52</sup> These are obtained from Intrinsic Atomic Orbitals (IAOs), a minimal set of atomic orbitals on atoms in molecules, polarised to depict the molecular environment. The IBOs obtained from IAOs represent chemical bonding, as commonly understood, even in difficult-to-

understand molecules. These localized bond vorbitals are generated using IBOview and represented for selected bord orbitals of 1, 2 and 3 (Figure 5). The localization identifies several obvious two-centre, two-electron bond orbitals and multicentre bond orbitals (Figures S31-33). Notably, the metal lone pair (Figure 5b), the three centre-two electron orbitals corresponding to bridging of B-B bonds with hydrogens (Figure 5c), and three multicentre orbitals connecting the Cp\* ring to the metal, remain consistent across all three complexes (Figures S31-33). Most intriguing variation is the nature of osmiumboron multicenter bond orbitals as we go from B<sub>6</sub> ring in 1 to B<sub>5</sub> and B<sub>4</sub> chains in 2 (Figure 5i), and 3 (Figure 5k), respectively. There are five multicenter bond orbitals involving the osmium and boron atoms (Figures 5d-h for 1, Figures S32 and S33 for 2 and 3). In 2 and 3, one of the multicenter bond orbitals has contributions from osmium, terminal boron and the hydrogen bridging them (Figures 5j and 5l). In 2, the terminal boron is bonded to four hydrogen atoms; two of these are terminal hydrogens, one forms a bridging bond with another boron, and one bridges between osmium and boron. This bonding environment classifies it as a [BH<sub>4</sub>] fragment. Notably, the B-H bond that interacts with osmium is considerably lengthened, and the osmium's interaction with this terminal boron is relatively weak (with B-H, Os-H and Os-B bond distances of 1.482 Å, 1.657 Å, and 2.324 Å, and corresponding bond orders of 0.36, 0.35 and 0.32, respectively). This weakened bond facilitates an easier transfer of hydrogen to another terminal boron (Figure 3). In contrast, in 3, the terminal boron is attached to three hydrogens; a single terminal hydrogen, one bridging bond with another boron, and one bridging between the osmium and boron-thus assigned as a [BH3] fragment. Here, the interacting B-H bond shows only minor elongation, and the osmium has a more pronounced interaction with both the boron and the hydrogen (with bond distances for B-H, Os-H, and Os-B being 1.339 Å, 1.797 Å, and 2.015 Å, and bond orders of

Table 1. Comparison of NICS values for  $[Cp^*Os(\eta^6-B_6H_{11})]$  (1) and bis(benzene)chromium  $[(C_6H_6)Cr(C_6H_6)]$  and  $[Cp^*OsCp^*]$ , computed at the B3LYP-D3/Def2-SVP level of theory. Negative NICS values imply aromaticity. In double-decker sandwich complexes, NICS(1.0) and NICS(-1.0) are measurements towards and away from the metal, respectively; see drawing on the left.



Complexes	NICS <sub>iso</sub> (0.0)	NICS <sub>zz</sub> (0.0)	NICS <sub>iso</sub> (1.0)	NICS <sub>zz</sub> (1.0)	NICS <sub>iso</sub> (-1.0)	NICS <sub>zz</sub> (-1.0)
[Cp*Os( $\eta^6$ -B <sub>6</sub> H <sub>11</sub> )], <b>1</b>	-37.6	-55.4	-49.5	-166.7	-11.4	-22.1
[(C <sub>6</sub> H <sub>6</sub> )Cr(C <sub>6</sub> H <sub>6</sub> )] <sup>53</sup>	-48.9	-58.3	-180.0	-229.7	-19.8	-34.0
[Cp*OsCp*] <sup>55</sup>	-25.9	-30.3	-73.2	-88.2	-12.9	-29.0

0.58, 0.26, and 0.73, respectively). This arrangement characterizes the interaction of a [BH<sub>3</sub>] fragment with an intact B–H bond as an agostic interaction, as described before.

# **Aromaticity Comparison**

We have further compared the aromaticity of the stabilized planar  $B_6$  ring in the monometallic template (1) with that of the benzene ring in bis(benzene)chromium,  $[(C_6H_6)C_7(C_6H_6)]^{53}$  (Table 1) using NICS values. While the absolute NICS values as indicators of aromaticity fail in metal complexes, a comparison

can be made between a series of related complexes.<sup>54</sup> NICS values follow similar trends for  ${\bf 1}$  and bis(benzene)chromium. It remains negative at the center and at positions 1 Å above (towards the metal) and below (opposite to the metal) the plane (see picture). The negative values away from the metal suggest  ${\bf 1}$  to be aromatic. Therefore, the planar  $B_6$  ring follows a similar aromaticity pattern of the benzene ring stabilized in double-decker sandwich complexes. The orbital interaction diagram (Figure 4, above) shows that despite the  $\sigma$ - $\pi$  mixing arising from bridging hydrogens in  $[B_6H_{11}]$ , the frontier MOs of

ARTICLE Journal Name

#### **Conclusions**

Synthesis of mixed metallocene, [Cp\*Os- $(\eta^6-B_6H_{11})$ ] (1), nido $arachno-[Cp*Os(n^5-B_5H_{12})]$  (2) and  $nido-arachno-[(Cp*Os)(n^4-B_5H_{12})]$ B<sub>4</sub>H<sub>9</sub>)] (3) from B<sub>1</sub> precursor [BH<sub>3</sub>·SMe<sub>2</sub>] presents novel possibilities in boron chemistry. In complex 1, five bridging hydrogens contribute to an 18-electron count configuration. In complex 2, four bridging hydrogens, along with an additional hydrogen bridging the Os-B bond, achieve the same 18electron count. In complex 3, although only three bridging hydrogens are present, a B-H bond donates two electrons to osmium in a manner similar to agostic sigma-complex formation, fulfilling the 18e configuration. These complexes also follow the mno rule. These novel ways in which [B<sub>6</sub>H<sub>11</sub>], [B<sub>5</sub>H<sub>12</sub>] and [B<sub>4</sub>H<sub>9</sub>] provide five electrons lead to dynamic degenerate rearrangements involving H-migrations that cannot be frozen even at low temperatures. Detailed analysis of aromaticity using NICS values shows that  $[Cp*Os(\eta^6-B_6H_{11})]$  is nearly as aromatic as bis(benzene)chromium,  $[(C_6H_6)Cr(C_6H_6)]$ . These findings emphasize the intricate bonding environments in all the complexes, with multicentre interactions playing a pivotal role in stabilizing the structures and opening up new approaches in organometallic chemistry without carbon.

## **Author contributions**

K. K. has executed the experimental synthesis, characterisation and analysed the data. G. J. has carried out theoretical calculations. All authors have contributed to the preparation of the manuscript. S. G. and E. D. J. have supervised the experimental and theoretical studies.

## **Conflicts of interest**

There are no conflicts to declare.

## Data availability

The data that support the findings of this study are available in the ESI† of this article.

# **Acknowledgements**

The generous support of SERB, New Delhi, India (grant no. CRG/2023/000189) is gratefully acknowledged. K. K thanks DST-INSPIRE, and G. J. thanks IISc for research fellowships. EDJ thanks ANRF for research funding through National Science Chair. We thank Dr. P. K. Sudhadevi Antharjanam and Dr. Babu Varghese, IIT Madras, for the single crystal X-ray diffraction data collection, structure refinement and discussion. The computational facility of SERC-IISc is gratefully acknowledged.

## **Notes and references**

View Article Online 0.1039/D5SC06992K

- O. J. Scherer, H. Sitzmann and G. Wolmershäuser, *Angew. Chem. Int. Ed.*, 1985, **24**, 351–353.
- E. Peresypkina, A. Virovets and M. Scheer, Coord. Chem. Rev., 2021, 446, 213995.
- 3 Z.-C. Wang, L. Qiao, Z.-M. Sun and M. Scheer, *J. Am. Chem. Soc.*, 2022, **144**, 6698–6702.
- 4 E. Urnėžius, W. W. Brennessel, C. J. Cramer, J. E. Ellis and P. v. R. Schleyer, *Science*, 2002, **295**, 832–834.
- 5 G. Joshi, M. N. Sreerag, E. D. Jemmis and J. F. Nixon, *Inorg. Chem.*, 2022, **61**, 15822–15830.
- 6 O. J. Scherer, H. Sitzmann and G. Wolmershäuser, *Angew. Chem. Int. Ed.*, 1989, **28**, 212–213.
- Y.-H. Xu, X. Yang, Y.-N. Yang, L. Zhao, G. Frenking and Z.-M. Sun, Nat. Chem., 2025, 17, 556–563.
- M. Lein, J. Frunzke and G. Frenking, Angew. Chem. Int. Ed., 2003, 42, 1303–1306.
- J. Rienmüller, B. Peerless, S. Paul, F. Bruder, W. Wernsdorfer,
   F. Weigend and S. Dehnen, Nat. Chem., 2025, 17, 547–555.
- R. Yadav, A. Maiti, M. Schorpp, J. Graf, F. Weigend and L. Greb, Nat. Chem., 2024, 16, 1523–1530.
- 11 N. Schwarz, F. Bruder, V. Bayer et al., Nat. Commun., 2025, 16, 983.
- 12 S. Kar, A. N. Pradhan and S. Ghosh, in *Comprehensive Organometallic Chemistry IV*, vol. 9, ed. G. Parkin, K. Meyer and D. O'Hare, Elsevier, 2022, pp. 263–369.
- 13 J. Zhang and Z. Xie, Acc. Chem. Res., 2014, 47, 1623–1633.
- 14 F. Zheng, T. H. Yui, J. Zhang and Z. Xie, Nat. Commun., 2020, 11, 5943.
- 15 J. Poater, M. Solà, C. Viñas and F. Teixidor, *Angew. Chem. Int. Ed.*, 2014, **53**, 12191–12195.
- 16 R. Borthakur, K. Saha, S. Kar and S. Ghosh, Coord. Chem. Rev., 2019, 399, 213021.
- 17 S. Ghosh, B. C. Noll and T. P. Fehlner, *Dalton Trans.*, 2008, 371–380.
- 18 A. Yagi, H. Kisu and M. Yamashita, *Dalton Trans.*, 2019, **48**, 5496–5499.
- 19 H. Hogeveen and P. W. Kwant, *Tetrahedron Lett.*, 1973, 12, 1665–1668.
- 20 M. Malischewski and K. Seppelt, *Angew. Chem. Int. Ed.*, 2017, 56, 368–370.
- 21 V. T. Brice, H. D. Johnson and S. G. Shore, J. Am. Chem. Soc., 1973, 95, 6629–6635.
- 22 M. L. McKee, J. Phys. Chem., 1989, 93, 3426-3429.
- 23 T. Kupfer, H. Braunschweig and K. Radacki, *Angew. Chem. Int. Ed.*, 2015, **54**, 15084–15088.
- 24 N. N. Greenwood, C. G. Savory, R. N. Grimes, L. G. Sneddon, A. Davison and S. S. Wreford, J. Chem. Soc., Chem. Commun., 1974, 718–719.
- 25 R. Weiss and R. N. Grimes, J. Am. Chem. Soc., 1977, 99, 8087–8088.
- 26 H.-J. Himmel, *Angew. Chem. Int. Ed.*, 2019, **58**, 11600–11617.
- 27 W. Lu, Y. Li and R. Kinjo, J. Am. Chem. Soc., 2019, 141, 5164–5168.
- 28 W. Lu, D. C. H. Do and R. Kinjo, *Nat. Commun.*, 2020, **11**, 3370.
- 29 S. Shyamal, D. Chatterjee, K. Kar and S. Ghosh, *Inorg. Chem.*, 2024, **63**, 21838–21848.
- 30 S. Kar, S. Bairagi, G. Joshi, E. D. Jemmis, H.-J. Himmel and S. Ghosh, *Acc. Chem. Res.*, 2024, **57**, 2901–2914.
- 31 G. Joshi and E. D. Jemmis, *Chem. Eur. J.*, 2024, **30**, e202402410.
- 32 E. D. Jemmis, G. Subramanian and M. L. McKee, *J. Phys. Chem.*, 1996, **100**, 7014–7017.
- 33 N. Alexandrova and A. I. Boldyrev, *Inorg. Chem.*, 2004, **43**, 3588–3592.
- 34 Y.-J. Wang, L.-Y. Feng, M. Yan, C.-Q. Miao, S.-Q. Feng and H.-J. Zhai, *RSC Adv.*, 2022, **12**, 8617–8623.

**Journal Name ARTICLE** 

- 35 L.-S. Wang, Acc. Chem. Res., 2024, 57, 2428-2436.
- 36 S. Ghosh, A. M. Beatty and T. P. Fehlner, J. Am. Chem. Soc., 2001, **123**, 9188-9189.
- S. Kar, S. Bairagi, A. Haridas, G. Joshi, E. D. Jemmis and S. Ghosh, Angew. Chem. Int. Ed., 2022, 61, e202208293.
- W.-L. Li, L. Xie, T. Jian, C. Romanescu, X. Huang and L.-S. Wang, Angew. Chem. Int. Ed., 2014, 53, 1288-1292.
- 39 B. P. T. Fokwa and M. Hermus, Angew. Chem., Int. Ed., 2012, 51. 1702–1705.
- 40 K. Kar, S. Kar and S. Ghosh, Chem. Sci., 2024, 15, 4179-4186.
- 41 A. S. Weller, M. Shang and T. P. Fehlner, Organometallics, 1999, **18**, 53-64.
- 42 W. Trakarnpruk, I. H. Kryspin, M. A. Arif, R. Gleiter and R. D. Ernst, Inorg. Chim. Acta, 1997, 259, 197-202.
- C. Luz, K. Oppel, L. Endres, R. D. Dewhurst, H. Braunschweig and U. Radius, J. Am. Chem. Soc., 2024, 146, 23741-23751.
- X. Lei, M. Shang and T. P. Fehlner, Chem. Eur. J., 2000, 6, 2653-
- T. P. Fehlner, Organometallics, 2000, 19, 2643–2651.
- S. Aldridge, M. Shang and T. P. Fehlner, J. Am. Chem. Soc., 1998, **120**, 2586-2598.
- 47 E. D. Jemmis, M. M. Balakrishnarajan and P. D. Pancharatna, J. Am. Chem. Soc., 2001, 123, 4313-4323.
- A. C. Reddy, E. D. Jemmis, O. J. Scherer, R. Winter, G. Heckmann, G. Wolmershäuser, Organometallics. 1992, 11, 3894-3900.
- 49 E. J. Baerends, T. Ziegler, A. J. Atkins, J. Autschbach, D. Bashford, O. Baseggio, A. Bérces, F. M. Bickelhaupt, C. Bo, P. M. Boerritger et al., ADF, SCM, Theoretical Chemistry, Vrije Universiteit, Amsterdam, The Netherlands, 2021, https://www.scm.com
- 50 G. te Velde, F. M. Bickelhaupt, E. J. Baerends, C. Fonseca Guerra, S. J. A. van Gisbergen, J. G. Snijders and T. Ziegler, J. Comput. Chem., 2001, 22, 931-967.
- 51 G. Knizia, J. Chem. Theory Comput., 2013, 9, 4834–4843.
- 52 G. Knizia and J. E. M. N. Klein, Angew. Chem., Int. Ed., 2015, **54**, 5518–5522.
- 53 D. Seyferth, *Organometallics*, 2002, **21**, 2800–2820.
- 54 P. v. R. Schleyer, B. Kiran, D. V. Simion and T. S. Sorensen, J. Am. Chem. Soc., 2000, 122, 510-513.
- 55 M. O. Albers, D. C. Liles, D. J. Robinson, A. Shaver, E. Singleton, M. B. Wiege, J. C. A. Boeyens and D. C. Levendis, Organometallics, 1986, 5, 2321-2327.

View Article Online

**Shemical Science Accepted Manuscript** 

DOI: 10.1039/D5SC06992K

- Crystallographic data have been deposited with the Cambridge Crystallographic Data Centre as supplementary publication no CCDC- 2438685 (1), 2438887 (2), 2438789 (3). These data can be obtained free of charge from The Cambridge Crystallographic Data Centre via <a href="https://www.ccdc.cam.ac.uk/data\_request/cif">www.ccdc.cam.ac.uk/data\_request/cif</a>.
- The data supporting this article have been included as part of the SI. Supplementary information: Experimental procedures and characterization of all species and reaction products.